



Relationship model for the drilling parameters from a digital drilling rig versus the rock mechanical parameters and its application

Qi Wang^{1,2} · Hongke Gao^{1,2} · Bei Jiang^{1,2} · Jun Yang² · Zhijin Lv³

Received: 27 December 2017 / Accepted: 26 June 2018 / Published online: 7 July 2018
© Saudi Society for Geosciences 2018

Abstract

Measuring rock mechanical parameters is an essential step for support design in an underground project. To quickly obtain the surrounding rock mechanical parameters at a construction site in real time using a digital drilling rig, a quantitative relationship between the drilling parameters and rock mechanical parameters should be defined. In this paper, based on the fracture characteristics of rock cutting, a relationship model for the drilling parameters of the digital drilling rig versus the rock mechanical parameters (DP-RMP model) is created. Based on the multi-function rock drilling test system developed by the authors, rock drilling tests for different drilling parameters and theoretical results are compared and analysed to prove the validity and accuracy of the DP-RMP model. Additionally, the influence laws of the cohesion and internal friction angle on the rock cutting drilling torque are investigated. Drilling parameters from the digital drilling rig-based rock mechanical parameter inversion method is proposed; the feasibility of this method is verified by rock drilling test results. The study provides a theoretical basis for quickly obtaining the rock mechanical parameters using drilling parameters on site in real time.

Keywords Digital drilling rig · Rock cutting · Drilling parameter · Rock mechanical parameter · Relationship model · Inversion method

Introduction

The testing of surrounding rock mechanical parameters such as the uniaxial compressive strength, cohesion and internal friction angle of an underground project is the basis for analysing the stability of surrounding rock and designing the support scheme. Tests for determination of strength parameters can be classified as the laboratory test method and the field test method. Currently, a point load test is the primary method to test rock strength on site; however, it cannot measure the rock cohesion and internal friction angle. Another option is to test the rock using a laboratory test, which takes

a long time and has a high cost. The digital drilling rig (Chen and Yue 2015; Gui et al. 2002; Kahraman et al. 2003) is a field survey device that provides accurate control and monitoring of the drilling parameters during drilling. Study results of numerous researchers show an obvious correlation between the drilling parameters of the digital drilling rig and rock mechanical parameters in the rock drilling process (Huang and Wang 1997; Patel 2013; Somerton 1959; Schunnesson 1996; Teale 1965). The prediction of rock mechanical parameters using the drilling parameters of the digital drilling rig has potential. In addition, the digital drilling rig provides a new way for quickly obtaining rock mechanical parameters using drilling parameters on site in real time. The key is to establish the quantitative relationship between the rock mechanical parameters and the drilling parameters.

Numerous researchers have conducted experimental studies and developed relationships among drilling parameters, such as the drilling rate, rotational speed and torque and rock mechanical parameters using statistics (Aalizad and Rashidinejad 2012; Mostofi et al. 2011; Yaşar et al. 2011). Song et al. (2011) performed a rotary penetration test for a material such as a wall building block and gypsum using a corner plate drill bit to investigate the relationship between the

✉ Qi Wang
chinawangqi@163.com

¹ Research Center of Geotechnical and Structural Engineering, Shandong University, Jinan 250061, China

² Key Laboratory for Geo-mechanics and Deep Underground Engineering, China University of Mining and Technology, Beijing 100083, China

³ Taiyuan University of Technology, Taiyuan 030024, China

rotary penetration parameter and the rock mechanical parameter. Yue et al. (2004) developed the drilling process monitor (DPM) and deployed it in Hong Kong weathered volcanic rock; it showed that the drilling rate of an impact rotary cutting drilling rig for the same homogeneous and continuous rock mass was fixed. Tan et al. (2008) discovered by field drilling tests that monitoring parameters such as effective axial pressure, drilling tool rotational speed and penetration rate had excellent responses to the rock strength variation at the boundary. Additionally, some researchers conducted preliminary studies on mechanical parameters during the rock cutting process using numerical simulations (Rojek et al. 2011; Su and Akcin 2011; Wyk et al. 2014).

In order to investigate the relationship between the drilling parameters and the rock mechanical parameters, a rock cutting mechanical model should be developed to deeply reveal the essence of the drill bit rock cutting mechanism and the relationship between the drilling parameters and rock mechanical parameters. This can provide a theoretical basis for obtaining the rock mechanical parameters on site using an inversion of the drilling parameters. Based on the equilibrium theory for axial force and torque work and the rock cutting energy during the drilling process, Karasawa et al. (2002a, b) derived a formula for rock drill-ability strength and drilling rig torque and axial force that described the relationship between the uniaxial compressive strength and drilling parameters. Based on the Mohr–Coulomb criterion, Nishimatsu (1972) derived a formula for the cutting force and rock mechanical parameter in the plane. Song et al. (2010) introduced a cutting rock mechanism to analyse the stress on the corner plate drill bit cut edge and created a mathematical model for the drill bit axial load, torque and rock and soil mechanical parameters. Although a relationship between the drilling parameters and rock mechanical parameters has been partially studied, the above models have a specific application range. Additionally, due to the complexity of the rock cutting process, rock mechanical parameters such as internal friction angle and cohesion cannot be obtained by inversion of the existing rock cutting theory of the drill bit for the digital drilling rig.

Based on existing studies, a relationship between the drilling parameters and rock mechanical parameters based on the fracture characteristics of rock cutting is analysed in this paper. A relationship model for the drilling parameters of the digital drilling rig versus the rock mechanical parameters (DP-RMP model) is created. Rock drilling tests are performed to verify the validity and accuracy of this model. Additionally, the influence laws of the cohesion and internal friction angle of rock on the drilling torque are investigated to reveal the response mechanisms of the drilling parameters to the rock mechanical parameters. A method to obtain the rock mechanical parameters by inversion of the drilling parameters of the digital drilling rig is proposed. Based on rock drilling test results, the feasibility of this method is verified. This method

provides a basis for obtaining the rock mechanical parameters from the drilling parameters dynamically on site and optimising the supporting parameters.

Analysis of rock cutting theory of drill bit for digital drilling rig

Analysis of rock cutting mechanical model

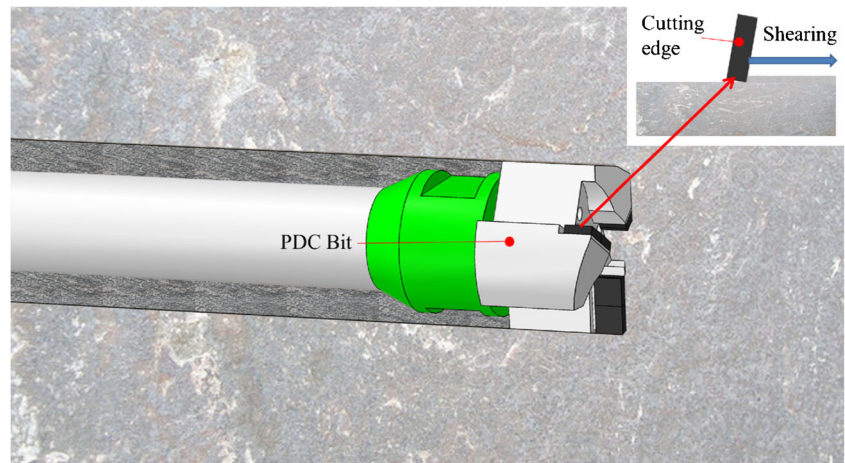
The rock cutting is performed using conventional polycrystalline diamond compact (PDC) drill bits, wherein the PDCs are embedded in a matrix to form cutting edges that crush rock, as shown in Fig. 1. Jaime et al. (2015) found that the forces fluctuate about a constant mean value for the shallow cut, and the cutting induces a plastic failure in the sample. Therefore, in this paper, aiming at the plastic failure mode of rock cutting, the rock cutting mechanical model of the drill bit for the digital drilling rig is created, as shown in Fig. 2. The assumptions are as follows:

1. The cutting width of the drill bit cutting edges far exceeds the cutting depth; the rock cutting problem is simplified to a plane strain problem.
2. Rock fragment cutting is completed instantaneously; the rock cracking surface reaches the ultimate bearing capacity at the same time.
3. The rock cracking surface is planar and follows the Mohr–Coulomb criterion; it has a horizontal inclination angle θ and extends to the free surface.

The rock cutting mechanical model of the drill bit for the digital drilling rig shows that when the drill bit PDC cutting edge rotates and penetrates into a rock, the front rock is under pressure, the pressure on the rock cracking surface reaches the shear strength and then shear failure occurs. In Fig. 2, F_s is the ultimate cutting load on the rock fragment from the drill bit cutting edge; P is a uniformly distributed constraint on the rock cracking surface, i.e., the resultant force of the ultimate shear stress τ_s and normal stress σ_n on the rock fragment along the cracking surface; θ is the shear angle; ψ is the angle between the cutting edge force on the rock fragment and the PDC normal, i.e., the ultimate cutting load inclination angle; γ is the cutting edge inclination angle; and the cutting depth of a single row cutting edge in one rotation is H .

Based on the rock cutting mechanical model of the drill bit for the digital drilling rig created in Fig. 2, the stress on an infinitesimal element of the rock fragment is analysed. Equilibrium requires that the resultant force from the integration of the uniformly distributed constraint P along the cracking surface be equal to the ultimate cutting load F_s . The ultimate shear stress and normal stress on the cracking surface are calculated to derive the ultimate cutting load.

Fig. 1 Three-dimensional schematic diagram of the PDC drill bit



The geometrical relationship between the two component forces σ_n and τ_s on the rock fragment cracking surface is

$$\sigma_n = \tau_s \tan(\theta + \gamma + \psi) \tag{1}$$

Based on the Mohr–Coulomb criterion,

$$\tau = c + \sigma \tan \varphi \tag{2}$$

where c is the cohesion and φ is the internal friction angle.

Let $\tau = \tau_s$ and $\sigma = \sigma_n$, and substitute Eq. (1) into Eq. (2), which becomes

$$\tau_s = \frac{c}{1 - \tan(\theta + \gamma + \psi) \tan \varphi} \tag{3}$$

Based on the geometrical relationship between the uniformly distributed constraint P and component force τ_s on the rock fragment cracking surface,

$$P = \frac{\tau_s}{\cos(\theta + \gamma + \psi)} \tag{4}$$

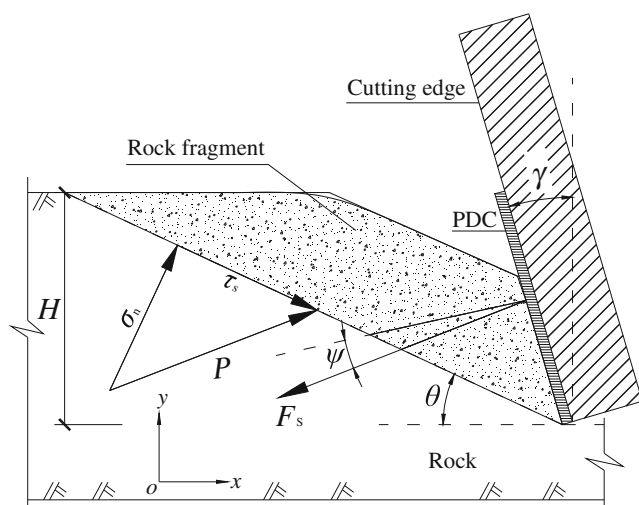


Fig. 2 Rock cutting mechanical model of drill bit for digital drilling rig

Therefore, the ultimate cutting load F_s is

$$F_s = \frac{PH}{\sin \theta} = \frac{\tau_s H}{\cos(\theta + \gamma + \psi) \sin \theta} \tag{5}$$

By substituting Eq. (3) into Eq. (5),

$$F_s = \frac{cH}{\cos(\theta + \gamma + \psi) \sin \theta - \sin(\theta + \gamma + \psi) \sin \theta \tan \varphi} \tag{6}$$

The derivative of θ in Eq. (6) is calculated. Let $\frac{\partial F_s}{\partial \theta} = 0$, so the ultimate shear angle is

$$\theta = \frac{1}{2} \left(\frac{\pi}{2} - \psi - \gamma - \varphi \right) \tag{7}$$

The ultimate shear angle in Eq. (7) is substituted into Eq. (6) to obtain the cutting edge ultimate cutting load F_s :

$$F_s = \frac{2cH \cos \varphi}{1 - \sin(\varphi + \gamma + \psi)} \tag{8}$$

The horizontal component of the force F_s is

$$F_{sx} = F_s \cos(\gamma + \psi) = \frac{2cH \cos \varphi \cos(\gamma + \psi)}{1 - \sin(\varphi + \gamma + \psi)} \tag{9}$$

where

$$H = \frac{V}{nN}$$

where V is the drilling rate, n is the number of drill bit cutting edge rows and N is the drill bit rotational speed.

Establishment of DP-RMP model

Based on the rock cutting mechanical model of the drill bit for the digital drilling rig, the drill bit force during the drilling process when the drill bit interacts with the rock is analysed, as shown in Fig. 3.

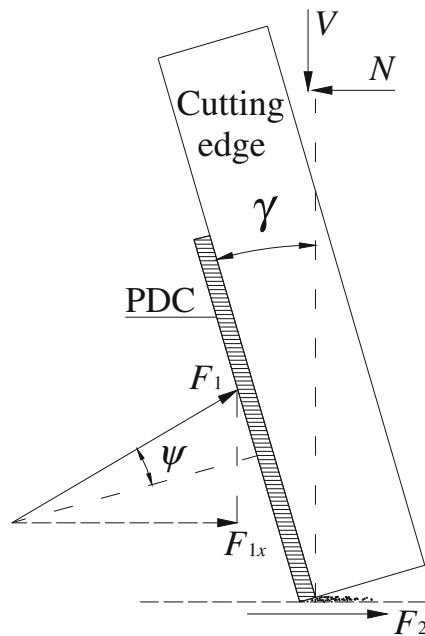


Fig. 3 Drill bit force analysis during the rock cutting process

Figure 3 shows that the drilling torque of the drill bit is divided into two parts:

1. Moment— M_A generated by the horizontal component force F_{1x} of rock cutting reacting force F_1 of the PDC cutting edge and
2. Moment— M_B generated by the friction force F_2 due to the cutting edge PDC bottom and rock interaction.

Therefore, the drilling torque M during the rock cutting process is

$$M = M_A + M_B \tag{10}$$

(1) Moment M_A calculation

Figure 4 shows the section dimension and cutting edge diagram of the drill bit used in the tests. The distance from a section of a row of cutting edges to the centre of the drill bit O is r , and the length of an infinitesimal segment is dr . The moment dM_A generated by the load from this infinitesimal segment on the drill bit centre is

$$dM_A = F_{1x}rdr \tag{11}$$

Integration of the infinitesimal segment moment dM_A along the length is calculated. The moments generated by F_{1x} from three rows of cutting edges are summed to obtain moment M_A :

$$M_A = \sum_{i=1}^3 \int_{r_i}^R F_{1x}rdr = \sum_{i=1}^3 \int_{r_i}^R F_{sx}rdr \tag{12}$$

$$= \frac{cH \cos \varphi \cos(\gamma + \psi)}{1 - \sin(\varphi + \gamma + \psi)} [2R(L_1 + L_2 + L_3) - (L_1^2 + L_2^2 + L_3^2)]$$

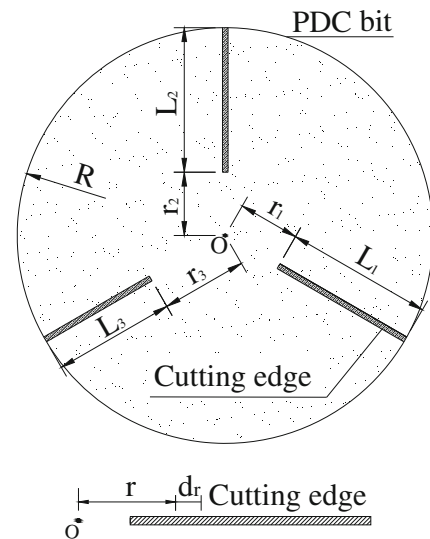


Fig. 4 Section dimension and cutting edge diagram of drill bit used in tests

where R is the drill bit radius, L_i ($i = 1, 2, 3$) represents the length of the i th row of the cutting edge and $r_i = R - L_i$. Based on the research results of Huang et al. (2013) and $\gamma = 15^\circ$ of the drill bit used in the tests, ψ was selected as 12° .

(2) Moment M_B calculation

When the drill bit rotates downward and cuts, the PDC crushes the rock at the bottom of the hole, and the underside of the PDC interacts with the rock at the bottom of the hole and generates sliding friction. In this paper, the compressive strength at the bottom of the PDC during the drill bit rotational cutting is the uniaxial compressive strength. According to the Mohr–Coulomb criterion, the uniaxial compressive strength of rock is $\sigma_c = 2c \cos \varphi / (1 - \sin \varphi)$. Therefore, F_2 is

$$F_2 = \mu \sigma_c e (L_1 + L_2 + L_3) = \frac{2c\mu e \cos \varphi (L_1 + L_2 + L_3)}{1 - \sin \varphi} \tag{13}$$

Therefore, the moment M_B is

$$M_B = \frac{F_2}{L_1 + L_2 + L_3} L_1 \left(R - \frac{L_1}{2} \right) + \frac{F_2}{L_1 + L_2 + L_3} L_2 \left(R - \frac{L_2}{2} \right) + \frac{F_2}{L_1 + L_2 + L_3} L_3 \left(R - \frac{L_3}{2} \right) \tag{14}$$

$$= \frac{F_2 [L_1(2R - L_1) + L_2(2R - L_2) + L_3(2R - L_3)]}{2(L_1 + L_2 + L_3)}$$

$$= \frac{c\mu e \cos \varphi}{1 - \sin \varphi} [2R(L_1 + L_2 + L_3) - (L_1^2 + L_2^2 + L_3^2)]$$

where μ is the friction coefficient between the PDC and the rock, based on the research results of Yahiaoui et al. (2016) and the characteristics of the drill bit used in this paper, letting

$\mu = 0.21$, and e is the thickness of PDC.

Based on the above calculation and analysis, the moments M_A and M_B in Eqs. (12) and (14), respectively, are substituted into Eq. (10) to create the DP-RMP model:

$$M = \left[\frac{cV \cos \varphi \cos(\gamma + \psi)}{3N[1 - \sin(\varphi + \gamma + \psi)]} + \frac{c\mu e \cos \varphi}{1 - \sin \varphi} \right] [2R(L_1 + L_2 + L_3) - (L_1^2 + L_2^2 + L_3^2)] \quad (15)$$

Rock drilling tests and verification

Test planning

(1) Test instrument

To verify the validity and accuracy of the DP-RMP model and define a quantitative relationship between the drilling parameters of the digital drilling rig and rock mechanical parameters, a multi-function rock drilling test system was developed by the authors, as shown in Fig. 5. This system includes a drilling system, a loading system, a pressure chamber device and a monitoring control system. It can test the correlation between the drilling parameters and rock mechanical parameters under various control modes. The drill bit used in the test is a new type of PDC drill bit, as shown in Fig. 5. A rectangular PDC is embedded into the cutting edge of this drill bit, which matches the assumptions of this paper. The drill bit parameters are listed in Table 1.

(2) Test material

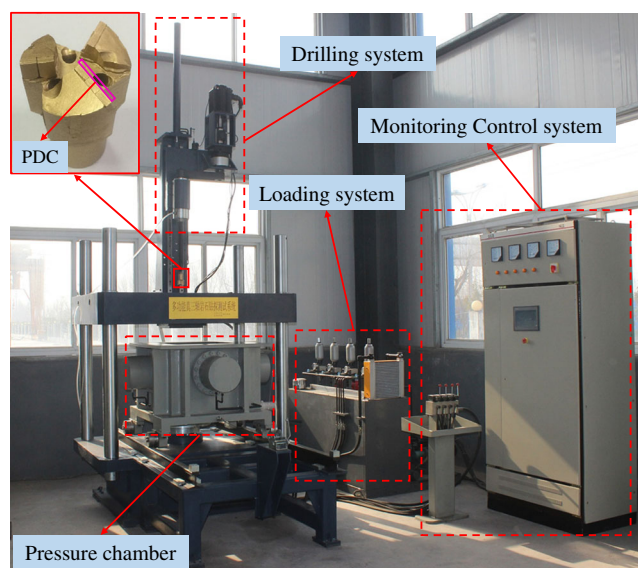


Fig. 5 Multi-function rock drilling test system and new type of PDC drill bit

Table 1 Parameters of the new type of PDC drill bit used in tests

Bit parameters	R	L_1	L_2	L_3	γ	e
Sizes	30 mm	18 mm	18 mm	27 mm	15 °	1.5 mm

Granite, limestone and sandstone specimens are used as test materials, with dimensions of $150 \times 150 \times 200$ mm (length \times width \times height). All specimens of the same lithology are cut and polished from the same batch of rock. Rock specimens before and after the test are shown in Fig. 6.

The rock mechanical triaxial test is performed on the rock specimens to obtain the basic mechanical parameters, which are listed in Table 2.

(3) Test schemes

The test mode to control the drilling rate V , rotational speed N and monitoring torque M is used. Drilling tests on granite, limestone and sandstone specimens at different drilling rates



Fig. 6 Rock specimens before and after the test

Table 2 Basic mechanical parameters of the rock specimens

Lithology	Cohesion, <i>c</i> (MPa)	Internal friction angle, φ (°)	Uniaxial compressive strength, σ_c (MPa)
Granite	16.5	48.1	86.3
Limestone	14.9	46.7	75.2
Sandstone	11.6	39.5	49.8

and rotational speeds are performed. Eighteen combinations are designed and numbered as *Gi*, *Si* and *Ki* (*i* = 1–6). The detailed schemes of the parameter settings are listed in Table 3.

Rock drilling test result selection

The variabilities of drilling torque versus drilling depth in test G1 are shown in Fig. 7. The graphs show that the drilling torque during the rock drilling process is divided into three stages:

- 1 Initial stage: Before the drill bit reaches the rock, because of the friction between the drilling rig system components, drill bit idling will generate stable initial torque.
- 2 Rising stage: When the drill bit reaches the rock, the drilling torque rises rapidly because of the PDC cutting rock process.

Table 3 Detailed test schemes of drilling tests for the granite, limestone and sandstone specimens

Lithology	No.	<i>V</i> (mm/min)	<i>N</i> (r/min)
Granite	G1	30	100
	G2	30	200
	G3	50	200
	G4	60	100
	G5	80	200
	G6	80	300
Limestone	S1	30	200
	S2	60	200
	S3	80	200
	S4	80	250
	S5	80	300
	S6	90	200
Sandstone	K1	30	100
	K2	30	200
	K3	60	200
	K4	80	200
	K5	110	200
	K6	140	200

No. represents the number of the test scheme. *V* represents the drilling rate. *N* represents the rotational speed of the drill bit

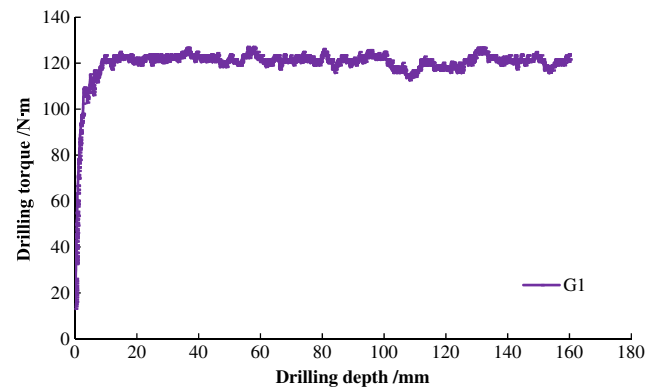


Fig. 7 The variation of drilling torque versus drilling depth in test G1

- 3 Steady stage: When the drill bit penetrates the rock and reaches a certain depth, the drilling torque rises to the required rock cutting torque. As the drill bit progresses further, the torque gradually stabilises. Due to the non-uniformity of the rock specimen material, the torque fluctuates in a narrow range until the test is ended.

The average torque of the steady stage minus the initial torque is the drilling torque *M* of this specimen. The average torque of the three specimens in each plan is defined as the drilling torque for this combination. Using plan G1 in Fig. 7 as an example, the specimen torque in the steady stage is 120.37 N m, and the initial torque is 15.72 N m. Therefore, the drilling torque of this specimen is 104.65 N m. The overall torques for the other two specimens in this test are 106.86 and 106.28 N m. Therefore, the drilling torque for this test is 105.93 N m.

Comparison of results from theoretical calculation and drilling tests

To verify the validity and accuracy of the DP-RMP model, rock drilling tests and theoretical results for schemes G1, G3, G5, S1, S3, S5, K1, K3 and K5 are compared and analysed. The statistics of the monitored drilling parameters and theoretical drilling torque of the above nine groups of tests are shown in Table 4. Additionally, the drilling torque theoretical result deviation rate (TDR) index λ is established.

$$\lambda = \frac{|M_T - M_E|}{M_E} \times 100\%$$

where M_E is the experimental drilling torque and M_T is the theoretical drilling torque.

Figure 8 shows the comparison and analysis of the theoretical and experimental drilling torque. An analysis of the diagrams reveals that the theoretical drilling torque versus the experimental results for the granite, limestone and sandstone are consistent. The average and standard deviations of TDR indexes are 7.16 and 2.91%, respectively. This shows that the

Table 4 Statistics of rock drilling experimental and theoretical results

No.	V (mm/min)	N (r/min)	M_E (N m)	M_T (N m)	λ (%)
G1	30.26	100.10	105.93	103.33	2.45
G3	48.72	198.73	84.05	89.96	7.03
G5	76.35	198.74	109.71	122.48	11.64
S1	33.97	198.73	65.93	59.43	9.86
S3	82.47	198.80	98.26	103.68	5.52
S5	84.04	297.22	82.99	79.72	3.94
K1	33.52	100.26	40.75	44.37	8.88
K3	60.84	198.87	38.41	42.18	9.82
K5	113.86	199.03	59.55	62.68	5.26

No. represents the number of the test scheme. V represents the drilling rate. N represents the rotational speed of the drill bit. M_E represents the experimental drilling torque. M_T represents the theoretical drilling torque. λ represents the drilling torque theoretical result deviation rate (TDR) index

theoretical drilling torque calculated from the DP-RMP model is close to the experimental result. The deviation rate fluctuation is small, and the theoretical result deviation for each scheme is relatively stable. This comparison of the theoretical and experimental results proves the validity and accuracy of the DP-RMP model.

Investigation of influence of rock mechanical parameters on drilling torque

To obtain the drilling parameter variation laws for different rock mechanical parameters, the drilling torques for different cohesion c and internal friction angles φ are calculated based on the DP-RMP model, and the results are analysed. The response mechanisms of the drilling parameter to rock mechanical parameters are revealed.

The cohesion c is set to 5, 10, 15, 20 and 25 MPa, and the internal friction angle φ is set to 10, 20, 30, 40 and 50°. The drilling rate is set to $V = 30$ mm/min, and the rotational speed is set to $N = 100$ r/min. The relationships between the drilling

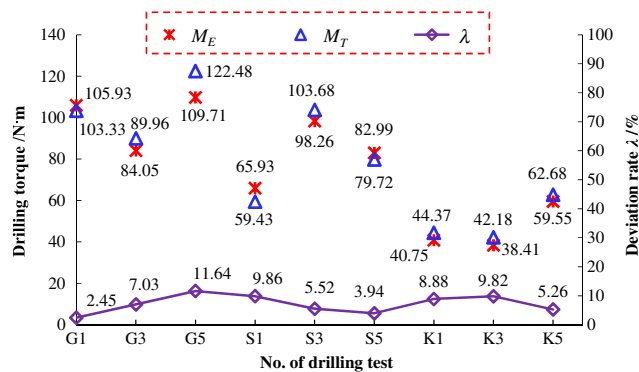


Fig. 8 Comparison and analysis of theoretical and experimental drilling torque

torque and the internal friction angle for different cohesion values and the drilling torque and cohesion for different internal friction angles are calculated, as shown in Figs. 9 and 10, respectively.

An analysis of Figs. 9 and 10 shows the following:

1. The drilling torque increases as the internal friction angle increases for different cohesion values, and the trend is consistent. A change in the internal friction angle has a significant impact on the torque. When the internal friction angle increases, the torque increases gradually during the initial stage and then rises rapidly.
2. The drilling torque increases as the cohesion increases for different internal friction angles, and the trend is consistent. A change in cohesion has a significant impact on the torque. The torque increases linearly as the cohesion increases.
3. The difference between the torque values when the cohesion and internal friction angle are both the maximal defined values and the minimal defined values is 179.1 N m. This difference is significant, which shows that rock hardness has a significant impact on the drilling torque. A higher level of rock hardness, i.e., higher rock shear strength and compressive strength, results in higher rock cutting torque, which matches the actual situation. Additionally, the results show that the rock mechanical parameters can be derived effectively from the drilling parameters of the digital drilling rig by inversion.

Application of the DP-RMP model

A method based on the DP-RMP model is proposed to derive the rock mechanical parameter from the drilling parameters of the digital drilling rig by inversion. The feasibility of this method is evaluated using a laboratory test. This provides

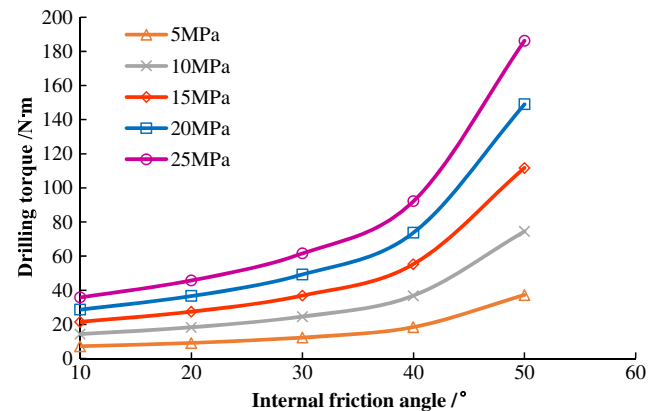


Fig. 9 The variation of drilling torque versus internal friction angle for different cohesion values

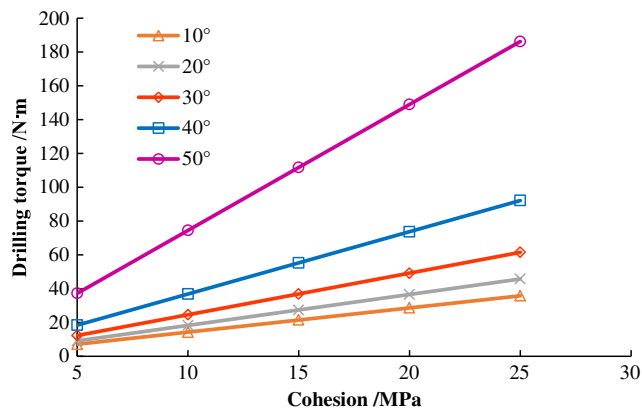


Fig. 10 The variation of drilling torque versus cohesion for different internal friction angles

the basis for obtaining the rock mechanical parameters on site in real time.

Establishment of method to derive rock mechanical parameters from drilling parameters by inversion

The DP-RMP model defines the quantitative relationship between the drilling torque and the rock internal friction angle and cohesion during drilling. A method based on the DP-RMP model to derive the rock mechanical parameters from the drilling parameters of the digital drilling rig by inversion is proposed in this paper. Based on the DP-RMP model and the uniaxial compressive strength formula in the Coulomb strength criterion, the rock internal friction angle and cohesion are calculated from the drilling torque M obtained from the rock drilling test and the uniaxial compressive strength σ_c obtained from the rock uniaxial test. Simultaneous equations for deriving the rock mechanical parameters from the drilling parameters of the digital drilling rig by inversion are shown in Eq. (16):

$$\begin{cases} M = \left[\frac{cV\cos\varphi\cos(\gamma + \psi)}{3N[1 - \sin(\varphi + \gamma + \psi)]} + \frac{c\mu\cos\varphi}{1 - \sin\varphi} \right] [2R(L_1 + L_2 + L_3) - (L_1^2 + L_2^2 + L_3^2)] \\ \sigma_c = \frac{2c\cos\varphi}{1 - \sin\varphi} \end{cases} \quad (16)$$

Verification of inversion method

To verify the validity of the method to derive the rock mechanical parameters from the drilling parameters by inversion, the rock mechanical parameter inversion results and triaxial test results for schemes G2, G4, G6, S2, S4, S6, K2, K4 and K6 are compared and analysed. The statistics of the monitored drilling parameters, cohesion and internal friction angle inversion results of the above nine groups of tests are shown in Table 5, where c_T denotes the cohesion inversion results and φ_T denotes the internal friction angle inversion results.

Table 5 Statistics of monitored drilling parameters and rock mechanical parameter inversion results

No.	V (mm/min)	N (r/min)	M_E (N m)	c_T (MPa)	φ_T (°)
G2	33.56	198.75	70.57	16.73	47.61
G4	61.34	99.85	161.17	17.11	46.74
G6	80.42	297.11	87.52	17.29	46.33
S2	58.61	198.76	87.97	14.44	47.97
S4	81.88	248.02	91.39	14.70	47.29
S6	91.16	198.62	117.09	14.64	47.45
K2	33.56	198.89	30.67	12.40	37.05
K4	85.48	198.80	51.05	11.98	38.62
K6	139.18	199.23	69.25	12.21	37.76

No. represents the number of the test scheme. V represents the drilling rate. N represents the rotational speed of the drill bit. M_E represents the experimental drilling torque. c_T represents the cohesion inversion results. φ_T represents the internal friction angle inversion results

- (1) Comparison of the rock cohesion inversion results versus the triaxial test results

A comparison of the cohesion inversion results versus the triaxial test results for the above nine groups of tests is shown in Fig. 11, and the rock cohesion drilling test inversion result deviation rate (CDR) index δ is established.

$$\delta = \frac{|c_T - c|}{c} \times 100\%$$

An analysis of Table 5 and Fig. 11 shows that the granite, limestone and sandstone test results are consistent, and the average CDR indexes of the above nine groups of tests are 3.50%. The differences between the cohesion drilling test inversion results and triaxial test results are small.

- (2) Comparison of the rock internal friction angle inversion results versus the triaxial test results

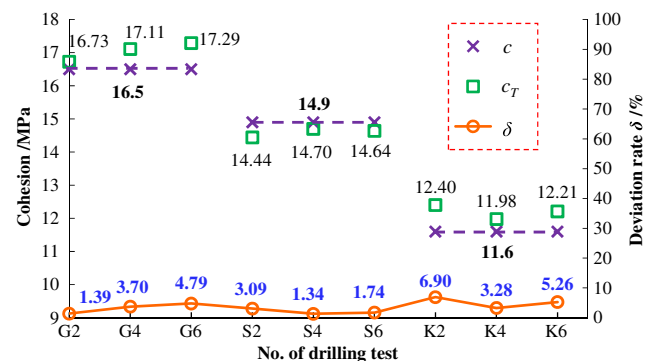


Fig. 11 Comparison of the rock cohesion inversion results versus the triaxial test results

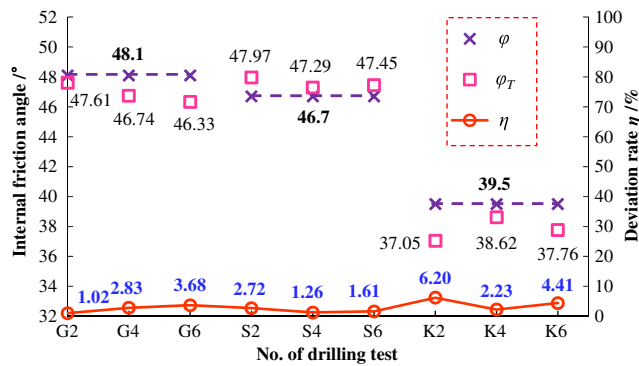


Fig. 12 Comparison of the rock internal friction angle inversion results versus the triaxial test results

A comparison of the internal friction angle inversion results versus the triaxial test results for the above nine groups of tests is shown in Fig. 12, and the rock internal friction angle drilling test inversion result deviation rate (IDR) index η is established.

$$\eta = \frac{|\varphi_T - \varphi|}{\varphi} \times 100\%$$

An analysis of Table 5 and Fig. 12 shows that, based on the method to derive the rock mechanical parameters from the drilling parameters of the digital drilling rig by inversion, the granite, limestone and sandstone test results are consistent, and the average IDR indexes of the above nine groups of tests are 2.88%. The differences between the internal friction angle drilling test inversion results and triaxial test results are small.

In summary, the CDR index and IDR index are less than 5%. This difference between the rock mechanical parameter drilling test inversion results and triaxial test results is small, which proves the feasibility of the method to derive the rock mechanical parameters from the drilling parameters of the digital drilling rig by inversion. The method provides a theoretical basis for quickly obtaining the rock mechanical parameters from the combined application of a digital drilling rig rock drilling test and a point load test for the actual project in real time.

Conclusions

(1) In this paper, based on the fracture characteristics of the rock cutting and characteristics of a new PDC drill bit developed by the authors, a relationship model for the drilling parameters from digital drilling rig and rock mechanical parameters (DP-RMP model) is established. Additionally, rock drilling tests and theoretical results for different drilling parameters are compared and analysed. The results show that the average TDR indexes are 7.16%, the standard deviations are 2.91%, the drilling

torque theoretical results are similar to the test results and the deviation rate fluctuation is small. This proves the validity and accuracy of the DP-RMP model.

- (2) The laws of influence of the cohesion c and internal friction angle φ on the drilling parameter are investigated. The result shows that the drilling torque is highly sensitive to rock mechanical parameters. When φ increases, the torque increases gradually during the initial stage and then rises rapidly in a non-linear pattern. When c increases, the torque increases linearly.
- (3) A method based on the DP-RMP model to derive the rock mechanical parameters from the drilling parameters of the digital drilling rig by inversion is proposed. The rock drilling tests and rock triaxial tests show that the CDR and IDR indexes are less than 5% and the differences between the drilling test inversion results and triaxial test results are small, which proves the feasibility of this method.
- (4) The DP-RMP model is established, and a method to derive the rock mechanical parameters from the drilling parameters of the digital drilling rig by inversion is proposed, providing a theoretical basis for quickly obtaining the rock mechanical parameters from the combined application of a digital drilling rig rock drilling test and a point load test for an actual project in real time.

Funding information This work was supported by the Natural Science Foundation of China (grant number 51674154), the China Postdoctoral Science Foundation (grant numbers 2017T100116, 2017T100491, 2016M590150, 2016M602144) and the Natural Science Foundation of Shandong Province, China (grant number 2017GGX30101).

References

Aalizad SA, Rashidinejad F (2012) Prediction of penetration rate of rotary-percussive drilling using artificial neural networks—a case study. *Arch Min Sci* 7(3):715–728

Chen J, Yue ZQ (2015) Ground characterization using breaking-action-based zoning analysis of rotary-percussive instrumented drilling. *Int J Rock Mech Min Sci* 75:33–43

Gui MW, Soga K, Bolton MD, Hamelin JP (2002) Instrumented borehole drilling for subsurface investigation. *J Geotech Geoenviron Eng* 128(4):283–291

Huang SL, Wang ZW (1997) The mechanics of diamond core drilling of rocks. *Int J Rock Mech Min Sci* 34(3–4):134.e1–134.e14

Huang H, Lecampion B, Detournay E (2013) Discrete element modeling of tool-rock interaction I: rock cutting. *Int J Numer Anal Meth Geomech* 37(13):1913–1929

Jaime MC, Zhou Y, Lin J, Gamwo IK (2015) Finite element modeling of rock cutting and its fragmentation process. *Int J Rock Mech Min Sci* 80:137–146

Kahraman S, Bilgin N, Feridonoglu C (2003) Dominant rock properties affecting the penetration rate of percussive drills. *Int J Rock Mech Min Sci* 40(5):711–723

Karasawa H, Ohno T, Kosugi M, Rowley JC (2002a) Methods to estimate the rock strength and tooth wear while drilling with roller-bits—part 1: milled-tooth bits. *J Ene Res Tech* 124(3):125–132

- Karasawa H, Ohno T, Kosugi M, Rowley JC (2002b) Methods to estimate the rock strength and tooth wear while drilling with roller-bits—part 2: insert bits. *J Ene Res Tech* 124(3):133–140
- Mostofi M, Rasouli V, Mawuli E (2011) An estimation of rock strength using a drilling performance model: a case study in blacktip field, Australia. *Rock Mech Rock Eng* 44(3):305–316
- Nishimatsu Y (1972) The mechanics of rock cutting. *Int J Rock Mech Min Sci* 9(2):261–270
- Patel A (2013) Characterization of cavities in rocks using drilling parameters. *Int J Rock Mech Min Sci* 63(5):122–130
- Rojek J, Oñate E, Labra C, Kargl H (2011) Discrete element simulation of rock cutting. *Int J Rock Mech Min Sci* 48(6):996–1010
- Schunnesson H (1996) RQD predictions based on drill performance parameters. *Tunn Undergr Sp Tech* 11(3):345–351
- Somerton WH (1959) A laboratory study of rock breakage by rotary drilling. *Trans AIME* 216:92–97
- Song L, Li N, Liu FY (2010) Study of mechanism of rotary penetration. *China J Rock Mech Eng (China)* 29(S2):3519–3525
- Song L, Li N, Li Q (2011) Study of intrinsic relationship between mechanical parameters and parameters of rotary penetration test of soft rock. *China J Rock Mech Eng (China)* 30(6):1274–1282
- Su O, Akcin NA (2011) Numerical simulation of rock cutting using the discrete element method. *Int J Rock Mech Min Sci* 48(3):434–442
- Tan ZY, Wang SJ, Cai MF (2008) Study on discriminant classification method for ground formation in identification of geotechnical engineering interfaces. *China J Rock Mech Eng (China)* 27(2):316–322
- Teale R (1965) The concept of specific energy in rock drilling. *Int J Rock Mech Min Sci* 2(1):57–73
- Wyk GV, Els DNJ, Akdogan G, Bradshaw SM, Sacks N (2014) Discrete element simulation of tribological interactions in rock cutting. *Int J Rock Mech Min Sci* 65(1):8–19
- Yahiaoui M, Paris JY, Delbé K, Denape J, Gerbaud L, Dourfaye A (2016) Independent analyses of cutting and friction forces applied on a single polycrystalline diamond compact cutter. *Int J Rock Mech Min Sci* 85:20–26
- Yaşar E, Ranjith PG, Viète DR (2011) An experimental investigation into the drilling and physico-mechanical properties of a rock-like brittle material. *J Pet Sci Eng* 76(3–4):185–193
- Yue ZQ, Lee CF, Law KT, Tham LG (2004) Automatic monitoring of rotary-percussive drilling for ground characterization—illustrated by a case example in Hong Kong. *Int J Rock Mech Min Sci* 41(4):573–612